Impact of metabolite accumulation on the structure, viability and development of succinic acid producing biofilms of *Actinobacillus succinongenes*

Sekgetho Charles Mokwatlo[a], Makhine Ernest Nchabeleng[a], Hendrik Gideon Brink[a], Willie Nicol[a]

[a]Department of Chemical Engineering, University of Pretoria, Lynnwood

Road, Hatfield, 0002, Pretoria, South Africa

Postal address: Department of Chemical Engineering, University of

Pretoria, Private Bag X20, Hatfield, 0028, South Africa

E-mail addresses:

Prof. W. Nicol: willie.nicol@up.ac.za : corresponding author

Dr H.G. Brink: deon.brink@up.ac.za

Mr. S.C. Mokwatlo: u11119072@tuks.co.za

Mr E.M. Nchabeleng: u12171736@tuks.co.za

Abstract

Biofilms of *Actinobacillus succinogenes* have demonstrated exceptional capabilities as biocatalysts for high productivity, titre, and yield production of succinic acid (SA). The paper presents a microscopic analysis of *A. succinogenes* biofilms developed under varied fermenter conditions. The concentration of excretion metabolites is controlled by operating the fermenter in a continuous mode where the liquid throughput is adjusted. It is clearly illustrated how the accumulation of excreted metabolites (concomitant with the sodium build-up due to base dosing) have a severe effect on the biofilm structure and physiology. Under high accumulation (HA) conditions some cells exhibit severe elongation while maintaining a cross sectional diameter like the rod/cocci shape cells predominantly found in low accumulation (LA) conditions. The elongated cells formed at high accumulation conditions were found to be more viable than the clusters of rod/cocci shaped cells and appear to form connections between the clusters. The global microscopic structure of the HA biofilms also differed significantly from the LA biofilms. Although both exhibited shedding after 4 days of growth, the LA biofilms were more homogenous (less patchy), thicker and with high viability throughout the biofilm depth. Viability of the HA biofilms were threefold lower than the corresponding LA biofilms towards the end of the fermentation. Visual observations were supported by quantitative analysis of multiple biofilm samples and strengthened the main observations. The work presents valuable insights on the effect of metabolite accumulation on biofilm structure and growth.

Keywords: *Actinobacillus succinogenes*; biofilms; succinic acid; biofilm viability; biofilm structure.

Introduction

Succinic acid (SA) is well established as a biobased platform chemical and has been commercially produced via fermentation since 2012 (Riverdia 2018; Nghiem et al. 2017). Currently succinic acid finds application in the pharmaceutical, food, and chemical industries (Song and Lee 2006). However, its most important application could potentially be as a replacement for maleic anhydride (due to similar chemical structures) and as a precursor for the intermediate 1,4-butanediol. Given that the majority of SA is currently produced petrochemically, through the catalytic hydrogenation of maleic anhydride derived from butane (Inkwood Research 2017), overwhelming research effort has gone into advancing possible bio-production processes for SA from biomass resources. The rapidly growing market for SA (Markets and Markets 2015) and the urgent need of switching to green technologies, in view of the advent climate change crisis, make the prospect of fermentative production of SA from renewable biomass resources desirable given that it stands to be a major production route for SA soon.

Among reported wild-type microbes for SA production—*Mannheimia succiniciproducens* (Lee et al. 2002), *Anaerobiospirillum succiniciproducens* (Samuelov et al. 1999), *Basfia succiniciproducens* (Scholten et al. 2009), and modified strains of *Escherichia coli* (Beauprez et al. 2010)—*Actinobacillus succinogenes* is one of the most promising strains. It has demonstrated a propensity to produce SA at high titre, yield and productivity in a mixed acid bench scale fermentation (Bradfield and Nicol 2014; Maharaj et al. 2014; Yan et al. 2014), well above its competitors. *A. succinogenes* is tolerant to high acid titres with reported high SA titres in literature ranging from 40 – 75 g L^{-1} (Marinho, Alvarado-Morales and Angelidaki, 2016; Ferone et al. 2018; González-García et al. 2018; Shen et al. 2018; Ki et al. 2008) , it also has an ability to utilise a wide range of carbon sources (Pateraki et al. 2016) including scalable

biorefinery streams (Zheng et al. 2009; Bradfield et al. 2015; Salvachúa et al. 2016). Moreover, its ability to unavoidably form biofilms (Maharaj et al. 2014), assists with stability in long term fermentation (Bradfield and Nicol 2014), improved tolerance to toxic substances (Bradfield et al. 2015), and attaining of high cell densities necessary for high SA volumetric productivities.

The production characteristics of SA with *A. succinogenes* biofilms have been studied extensively in the open literature; exploring steady-state metabolite distributions at varying glucose consumption rates (Maharaj et al. 2014; Bradfield and Nicol 2014; Urbance et al. 2004; Brink and Nicol 2014), rate and yield comparisons of biofilm and suspended cell fermentation (Maharaj et al. 2014; Brink and Nicol 2014), fermentations of various sugar types including hydrolysate streams (Ferone et al. 2018; Salvachúa et al. 2016; Bradfield et. al. 2015; Zheng et al. 2009), as well as using different reactor configuration schemes (Brink and Nicol, 2014; Urbance et al. 2004). It has consistently been observed that metabolite accumulation (which is concomitant with sodium build-up due to caustic dosing) in a fermenter inhibits cell growth (Maharaj et al. 2014; Bradfield and Nicol 2014; Brink and Nicol 2014; van Heerden and Nicol 2014), yet there is a continued production of metabolites. Brink and Nicol (2014) collated data from prominent batch studies comparing specific biomass growth rates against the SA titre (indicative of metabolite accumulation conditions), the resultant data cloud uncovered severe biomass growth inhibitions, with an eight-fold decrease in the specific biomass growth rate between SA concentrations of 0 to 7 g L^{-1}. As such, in high accumulation (HA) broth conditions, *A. succinogenes* enters a regime of considerably slow cell growth where mixed acid production is maintenance driven (Bradfield and Nicol 2014). van Heerden and Nicol (2013) mark this HA regime as being beyond SA titres of 10 g L^{-1}. Increased selectivity for SA with increasing metabolite production is reported in HA conditions (Bradfield and Nicol 2014). Moreover, contrary to low accumulation (LA) conditions where metabolite production is driven by cellular growth, there is a minimal loss of carbon to biomass in the HA conditions

due to negligible biomass growth, thus increased yields of SA are achieved, making the HA conditions a suitable place for SA production. In summary, *A. succinogenes* was shown to switch between two regimes where SA production is either driven by biomass growth or by maintenance of biomass with significantly reduced growth.

From a volumetric productivity perspective, bulk production of SA through fermentation should employ continuous high cell density bioreactors able to operate at high SA titres for extended periods. In this regard it is imperative to understand the interaction between the biofilm and the accumulation of the produced metabolites, as this will have impact on the stability of the process. This study addresses how the accumulation of metabolites interacts with the biofilm on the basis of its development, structure and viability in its early stage development and within the two regimes of growth and maintenance driven SA production. A comparison is thus made of *A. succinogenes* biofilms cultivated under both low accumulation conditions (less than 10 g L^{-1} SA) and high accumulation conditions (more than 10 g L^{-1} SA)— conditions which signify regimes of growth-driven and maintenance driven SA production by *A. succinogenes*, respectively. The global microscopic structure, cell morphology and viability of the biofilm are evaluated in each condition and compared to establish the role played by accumulation conditions. The global microscopic structure is further quantified using specific parameters in COMSTAT for consolidation of qualitative visual observations of microscopic images.

Materials and Methods

Microorganism and fermentation media

Wild-type *Actinobacillus succinogenes* 130Z (DSM No. 22257; ATCC No. 55618) was acquired from the German Collections of Microorganisms and Cell Cultures (Braunschweig,

Germany). Stock cultures (1.5 mL) were stored at -40 °C in 66% v/v glycerol solutions. Inoculum was prepared by transferring a stock culture to 100 mL of sterilised tryptone soy broth which was then incubated at 37 °C and 120 rpm for 16 − 24 h. High-performance liquid chromatography (HPLC) was used to determine the purity and viability of the inoculum by checking for consistent metabolite distribution prior to inoculation of the system.

The composition of the fermentation medium used was based on that of Bradfield & Nicol (2014). All chemicals were obtained from Merck KGaA (Darmstadt, Germany) unless otherwise stated. The medium was made up of three parts: the nutrient and salts solution, a phosphate buffer, and the glucose solution. The nutrient and salt solution was composed of (in g L^{-1}) 10.0 of clarified corn steep liquor (Sigma-Aldrich, St. Louis, USA), 6.0 of yeast extract, 0.5 NaCl, 0.2 $MgCl{\cdot}6H_2O$, 0.2 $CaCl_2{\cdot}2H_2O$, and 10 mL L^{-1} of antifoam SE-15 (Sigma-Aldrich, Germany). The phosphate buffer consisted of 3.2 g L^{-1} KH_2PO_4 and 1.6 g L^{-1} K_2HPO_4. The glucose concentration was kept at 60 g L^{-1}. CO_2 (Afrox, South Africa) was fed the fermenter at 0.1 vvm.

Experimental setup

The experimental setup used was adapted from Bradfield and Nicol (2014). A novel bioreactor suitable for sterile and multiple biofilm sampling was used. The bioreactor consisted of a middle section of a hollow aluminium cylinder which housed twelfth slots, three on each of the four sides, within which cylindrical aluminium rods carrying the biofilm sample coupon could be inserted. Each sample probe rod carried two sample coupons, refer to Fig. 1. Two 13 mm diameter Thermanox coverslips (Thermo Fisher Scientific, Massachusetts, USA) were temporarily affixed on each sampling probe prior to each run. The top and bottom of the middle hallow aluminium section were connected to a cylindrical glass, which allowed for an aluminium head—fitted at the centre with a shaft holding a Rushton 6 blade impeller for mixing

within the bioreactor— and an aluminium base to encase it. Four wooden sticks covered with mutton cloth were inserted in the fermenter to provide the attachment surface for sufficient and stable biofilm growth within the main fermenter body, only for HA biofilm cultivation. The total working volume of the fermenter was 3000 mL and it was maintained by means of an overflow tube (in the fermenter) connected to the exit pump. Temperature and pH were controlled at 37.0 ± 0.1 °C and 6.80 ± 0.01 respectively. A Liquiline CM442 (Endress+Hauser, Gerlingen, Germany) coupled to a Ceragel CPS71D glass electrode (Endress+Hauser, Gerlingen, Germany) measured both temperature and pH, and also controlled pH through an on and off dosing of a 10 M NaOH by using an internal relay. Temperature was controlled by a feedback PID controller, custom-developed in Labview. All gas vents and inlets were fitted with 0.2 µm PTFE membrane filters (Midisart 2000, Sartorius, Göttingen, Germany) to ensure sterility. Mixing in the bioreactor was kept at 300 rpm using a Rushton 6 blade impeller connected to an overhead stirrer.

Biofilm Cultivation

The entire experimental setup was autoclaved at 121 °C for 60 min excluding the NaOH reservoir. Prior to inoculation, the setup was left to run for a day to confirm sterility. Sample probes were inserted into their slots but isolated from the fermenting medium by clamping the silicon section of the isolation chambers. Sample probes were fully slotted into the bioreactor, aseptically, once the desired acid titre conditions were reached for biofilm cultivation. The bioreactor was operated in batch mode after inoculation (~100 mL). Acid concentrations were monitored during this batch mode and a switch to continuous operation was made at the desired acid titres. A switch to continuous mode was made at 21 g L^{-1} SA for HA biofilm cultivation at a low dilution rate of 0.05 h^{-1}, this dilution rate was maintained throughout the run, and the sample probes were fully slotted into the bioreactor immediately after switching to continuous

mode. Fig. 2 shows the metabolite titre profiles for the two experiments performed where the biofilm was cultivated at both HA and LA conditions. A preliminary experiment at LA conditions was also performed using a small version (630 mL) of the bioreactor. As it was expected that growth will be slow for HA biofilm cultivation, biofilm sampling was performed on day 1, 3 and 5 (counting from the day sample probes were inserted) so as to extend the period of growth. For LA growth, however, a switch to continuous mode was made at 8 g L^{-1} SA titre and a high dilution rate of 0.3 h^{-1} was maintained. Biofilm sampling was performed on day 1, 2, 3 and 4 as rapid growth of biofilm was anticipated. In the results section, a constant reference to LA and HA conditions is made, it should be noted that this refers to metabolite growth conditions shown in Fig. 2a and Fig. 2b respectively.

Biofilm image acquisition

After aseptic removal of sample probes, coverslip biofilm coupons were gently dislodged from the probes. Consequently, the coupons were immediately immersed in a phosphate buffered saline solution of pH 7.4 (at 37 °C) inside a six-well plate for 5 min. Coupons were gently rinsed twice with a PBS solution, and stained using Baclight LIVE/DEAD bacterial viability (Thermo Fisher Scientific, USA) stains at the recommended concentrations of stains. Samples were then incubated at 37 °C for 30 min in the dark. After staining, the samples were gently rinsed with distilled water and mounted on glass microscope slides.

Biofilm images were acquired using a Zeiss LSM 880 laser scanning confocal microscope (Zeiss, Germany). Biofilm samples were observed with 40× (Plan-Neofluar 40×/1.3 Oil DIC) and 100× (Plan-Apochromat 100×/1.4 Oil DIC) objectives. Image z-stacks were acquired by taking a series of horizontal *xy* optical scans from the substratum surface to the top of the biofilm section in set steps of 2 µm. The z-stack scans were acquired at random locations on the biofilm coupons. Only the 40× objective lens was used for acquiring z stacks to be used for

quantitative analysis. A minimum of 20 image z-stacks per day of sampling were acquired, ensuring that descriptive quantitative parameters of the biofilm are computed based on a biofilm sample area that is representative of the biofilm, as previously determined by Mokwatlo and Nicol (2017). An excitation wavelength of 488 nm was used and the emission fluorescence was collected at 635 nm and 500 nm.

Analytical Methods

Acquired biofilm images were post processed with a ZEN 2.3 Lite Image Processor (Zeiss, Germany) and ImageJ (Schneider et al. 2012) prior to quantitative analysis. A Comstat2 digital image analysis software, a plugin in ImageJ, was used to generate quantitative data of the acquired image z-stacks (Heydorn et al. 2000). The mean biofilm thickness (μm), biomass content of the biofilm (μm^3 biomass voxels per μm^2 surface area), biofilm surface to biofilm volume ratio, and the roughness co-efficient parameter were computed for each image stack. Quantitative biofilm viability results were compared using an unpaired t test with a confidence level of 95% using GraphPad Prism software (GraphPad Software, USA).

Concentrations of glucose, ethanol and organic acids in the fermenter broth were determined by High-Performance Liquid Chromatography (HPLC). An Agilent 1260 Infinity HPLC (Agilent Technologies, USA), equipped with an RI detector and a 300 mm × 7.8 mm Aminex HPX-87H ion exchange column (Bio-Rad Laboratories, USA) was used. Two mobile phases were used for two methods of analysis. The first method consisted of a 5 mM H_2SO_4 mobile phase solution fed at a flowrate of 0.6 mL min^{-1} and the second method used a 20 mM H_2SO_4 mobile phase at the same flowrate. The second method improved the accuracy of the glucose reading by separating the phosphate, glucose and pyruvic acid peaks.

Results

Impact of metabolite accumulation on cellular morphology

Actinobacillus succinogenes biofilm and suspended cells expressed a different morphology according to respective conditions the biofilm was cultivated in as shown in Fig. 3. Biofilm cells were cocci-shaped with a diameter of approximately 0.4 – 0.5 µm at the lowest SA titre of growth (average of 6.0 g L^{-1} over 4 days, preliminary experiment). The cells became rod-shaped (width of 0.4 – 0.5 µm and length of 1-2 µm) when biofilm was cultivated at average SA titres of 8.6 g L^{-1} (average SA titre over 4 days) as seen in Fig.3b. Severe biofilm cell filamentation (width of 0.4 – 0.5 µm and length of 5 – 200 µm) was witnessed at high SA titres of 15.9 g L^{-1} (average SA titre over 5 days), though cocci-shaped cells were still observed in the form of cell clusters in this concentration regime. Filamentation occurs as cells continuously grow yet do not undergo septation and thus do not divide. During this growth, biofilm cells maintain their cell width while increasing in length, causing a reduction in their surface area to volume ratio.

Impact of metabolite accumulation on biofilm development and structure

Low accumulation conditions biofilm development

Representative 3D *x-y* plane images profiling the biofilm development at LA conditions are shown in Fig. 4 as well as the *x-z* plane images showing the biofilm thickness profile. Biofilm growth was rapid when cultivated under low accumulation conditions, assenting that the conditions were favourable for biomass growth. In keeping with rapid growth, the substratum surface was completely covered by a basal layer of rod-shaped cells (2 – 4 µm) on the first day, and out of this layer protruded pillars of cell clusters with varying thickness—as can be seen by an uneven thickness profile in Fig. 4b (day 1)—some of which were as thick as 42 µm. The structure observed on the first day at low titre was thus that of a heterogeneous dispersion of

amorphous cell clusters. Day 2 and 3 images in Fig. 4(a&b) show that the biofilm became thicker and much uniform with regard to thickness across the colonised surface, as a result there was a disappearance of voids and the biofilm resembled a dense and thick layer of cells on day 3. On day 4 there was overall reduction in the thickness of the biofilm, this was due to an observed shedding of the biofilm as was seen by an increase in the biomass content of the bioreactor broth effluent.

High accumulation conditions biofilm development

Contrary to biofilm development at low accumulation conditions, the biofilm struggled to grow in high accumulation environments. After the first day of growth, the biofilm had developed into a patchy distribution of cell clusters which were interconnected by a branched network of long filamentous cells (Fig.5a), thus there was a low coverage of the substratum surface. Cell clusters, made up of cocci-shaped cells, had grown significantly in size and number by the third day and were thus closely spaced, resulting in a biofilm that is uniform with regard to thickness, as is shown in Fig. 5b. In addition, more filamentous cells were also observed, and these were mostly located in-between the borders of neighbouring cell clusters (Fig. 6, indicated by white circles). It was also observed that filamentous cells were protruding out of a cell clusters and entering other neighbouring cell clusters (Fig. 6, indicated by white arrows), and as such, they gave an impression that they were holding the cell clusters together. This observation was also noted by Janissen et al. (2015), who reported the filamentation of *Xylella fastidiosa* bacterial cells located on the borders of cell clusters in a biofilm and interconnecting cell clusters. It is possible that the elongated cells connecting cell clusters play a sensory role as they are much sensitive to environmental changes around them compared to cells within cell clusters. Interconnecting of cell clusters with filamentous cells may provide stability of the resulting biofilm structure. Nonetheless, by the fifth day, the biofilm looked patchy again as

most of the cell clusters had disintegrated from the biofilm (Fig 5.c), this was expected as cell clusters were mostly stained red (indicative of cell death) after 3 days of growth, and excessive shedding was witnessed on day 4 as seen by the increased biomass concentration of the broth effluent.

Quantitative comparison of LA and HA cultivated biofilms

A quantitative analysis of the biofilm z-stack images collected during the experiments was performed using COMSTAT to quantitatively compare biofilm parameters for biofilm grown in low and high accumulation environments. The exact same procedure for pre-processing the biofilm images prior to quantitative analysis was followed so to not introduce variability. The biomass content of the biofilm (μm^3 biomass voxels per μm^2 surface area), the exposed biofilm surface to biofilm volume area, the mean biofilm thickness, and the roughness co-efficient of the biofilm were compared. Results are shown in Fig. 7. Standard deviations of the computed parameters in Fig. 7 were quite significant, however this is a common observation in biofilm parameter quantification due to innate biofilm structure variability and is to be expected as an extensive biofilm area was sampled (minimum of 20 image z-stacks).

The quantitative data was consistent with observations made visually from microscopic images. Though both biofilms cultivated at low and high SA titre achieved a peak biomass content by the third day of cultivation, the biofilm cultivated at LA conditions gained biomass content more rapidly (a mean of 10 $\mu m^3/\mu m^2$/day vs 5 $\mu m^3/\mu m^2$/day) and achieved higher biomass content (Fig 7a) compared biofilms cultivated at HA conditions. A maximum mean biofilm thickness of 30 μm and 15 μm for low and high accumulation condition biofilm cultivations, respectively, were achieved on the third day. There was a decline in both the biomass content and biofilm thickness for both low and high accumulation biofilm cultivation

after the third day, giving evidence for the observed biofilm shedding (Fig. 7 a&c). The surface to volume to ratio of biofilms grown at LA was consistently lower than that of the biofilm grown at high titres, as is expected for a patchy biofilm structure (for HA conditions) versus a flat uniform one. As such, the roughness co- efficient, indicative of biofilm thickness variability, was higher for the patchy biofilm cultivated at high acid titres. Overall, the quantitative data results show that growth at both low and high accumulation conditions follow the same trend where there is an initial accumulation of biomass and an eventual shedding, however, biomass accumulation is markedly slow when biofilm is cultivated at high accumulation conditions.

Impact of metabolite accumulation on biofilm viability

Staining of the biofilm with SYTO9 and propidium iodide of the Baclight Bacterial Viability Kit allowed the discrimination of dead and living cells within the biofilm. Dead cells emitted red fluorescence whereas living cells emitted green fluorescence. To get an indication of the extent of the viability of the biofilm, a ratio of the mean intensity of the green fluorescence to the mean intensity of the red fluorescence for each *xy* plane of a z-stack was calculated. The green/red intensity ratios were further collated and averaged for all the z-stacks collected on the specific day of sampling, which allowed an observation how the overall biofilm viability varied as the biofilm developed (Fig. 8a). Henceforth the mean green/red intensity ratio is referred to as the viability factor. It must be noted that this was not an absolute value for viability but an indicator of the extent of the viability of the biofilm based on the averaged colour intensities. A viability factor of one approximates an equal distribution of dead and living cells, whereas decreasing viability factors below one approximates increasingly higher fraction of dead cells and increasing viability factors above one approximate increasingly

higher fractions of living cells. Fig. 8c gives *xy*-images of the biofilm with their viability factors for reference purposes.

The viability factor for biofilms cultivated under low accumulation conditions (average SA titres of 8.6 g L^{-1} over 4 days) increased from the first day to the third day and dropped slightly on the fourth day Fig. 8a. In contrast, the viability factor for the biofilm cultivated at high accumulation conditions decreased throughout its development. As such the viability of the HA biofilms was threefold lower than the corresponding LA biofilms towards the end of the fermentation. In this way, the biofilm became increasingly composed of a higher fraction of dead cells when cultivated at high acid titre environments, unlike when cultivated under low acid titre conditions where it became more and more composed of viable cells. A statistical comparison (student's t test) of viability factors for LA and HA for day 1 and 3 is given in Table 1. The LA grown biofilms had significantly high viability factors than HA grown biofilms, and this was more pronounced on the third day. Accumulation conditions thus caused statistical difference in the viability of biofilms.

The viability factor profile across the biofilm depth was also analysed for, using 3 day old biofilms for both low and high accumulation biofilm cultivation. The viability factor decreases as you go deeper into the biofilm towards colonisation surface for biofilm cultivated at low acid titres (Fig. 8b). For high accumulation biofilms, the viability factor peaked in the middle layer of the biofilm as the top and deeper layers of the biofilm had the lowest viability factor. It was also observed that the branched networks of filamentous cells, expressed in biofilms cultivated at high metabolite accumulation conditions (Fig 5b and Fig. 6), were mostly stained green. This indicated that filamentous cells were more tolerable to high metabolite accumulation conditions.

Discussion

The stability and activity of the biocatalyst biofilms of *Actinobacillus succinogenes* is critical to the prospect of bulk scale continuous fermentative production of SA. Unlike physical catalysts, biocatalysts will be impacted by the surrounding environmental conditions. This study is the first to investigate the impact of accumulation of metabolites, together with sodium due to pH control with caustic, on the development of the *A. succinogenes* biofilm by employing microscopic analysis. The results of this study show that biofilms of *A. succinogenes* develop rapidly and with high viability when cultivated under low metabolite accumulation conditions. This is consistent with observations by Maharaj et al. (2014), Brink and Nicol (2014) and van Heerden and Nicol (2014) who all reported rapid biofilm development in a continuous bioreactor at high dilution rates where accumulation is low. In contrast, very slow and low viability biofilms are observed when the biofilm is cultivated in high metabolite accumulation conditions. As per studies by Liu et al. (2008), it is possible that a significantly high concentration of the cation of the neutralising base, sodium, is responsible for the slowed growth. However, acid accumulation is also known to inhibit growth of *A. succinogenes*, according to studies by Pelayo-ortiz and Corona-Gonzalez (2008).

High dilution rate biofilm establishment was also reported to cause instabilities due to frequent biofilm shedding (Maharaj et al. 2014). In this study however, a single biofilm shedding event was observed for each of the growth conditions investigated within the chosen cultivation period. Thus, shedding appeared to be a natural occurrence in the development cycle of the biofilm as reported elsewhere (Costerton 1999) and it is expected that biofilms operated at high accumulation conditions will take much longer times to recover from shedding events due to slow growth observed in these conditions.

It is also shown that though biofilm development occurs at high accumulation conditions, it happens at a great cost to biofilm viability. This explains the loss in specific mass-based SA productivity at increasing metabolite accumulation conditions observed by both Brink and Nicol (2014) and Maharaj et al. (2014). The apparent loss in biomass-based SA productivity is due to the fraction of metabolically active cells within the biofilm decreasing with increasing metabolite accumulation conditions. Moreover, since biomass production depends on the number of active cells within the biofilm, it may well be that extensive cell death at high acid titres contributes much to the apparent slow/inhibited growth.

At a cellular level, *A. succinogenes* biofilm and suspended cells respond to increasingly HA broth conditions by becoming elongated. Moreover, cell elongation was much severe beyond the 10 g L^{-1} SA titre reported by Brink and Nicol (2014) as the onset of significant inhibition of cell growth for *A. succinogenes* fermentations. There has been reports of bacterial cells undergoing filamentation as a survival strategy to unfavourable conditions such as treatment with antimicrobial agents (Hwang and Lim 2015) and even high salinity environments (Jones et al. 2013). In this study however, it is yet uncertain whether the observed cell elongation was directly caused by the unfavourable conditions that resulted from the high acid concentrations or the increased salinity of the broth due to concomitant neutralisation of produced acids with NaOH for maintaining the broth pH. Nonetheless, it is evident that the elongated cell morphology confers the cell with tolerance to what would otherwise be harmful conditions as filamentous cells remained active at high accumulation conditions. Moreover, because of their tendency for entanglement, filamentous cells may improve the structural intactness of the biofilm and thus aid the stability of the biofilm.

Overall, in perspective of the industrial scale bio production of SA wherein it is likely that healthy biofilm is first cultivated before switching to SA production mode, the results suggest that the

cultivation step should be performed at low accumulation conditions where growth is rapid and occurs at high viabilities of the biofilm. Moreover, the apparent tolerance of filamentous cells to high metabolite accumulation conditions necessary for high volumetric productivity of SA, may be used to an advantage. It is proposed that by gradually decreasing the throughput, after biofilm cultivation at high throughputs, a slow metabolite accumulation will result thus allowing rod-shaped cells in the previously developed biofilm to filament. This will possibly result in biofilm composed of filamentous cells able to tolerate operation at high metabolite accumulation without significant loss in biofilm viability.

Acknowledgements

The Laboratory for Microscopy and Microanalysis at the University of Pretoria is acknowledged for their assistance with the microscope equipment. The financial assistance of the Sugar Milling Research Institute via the Step-Bio program is hereby gratefully acknowledged. The financial assistance of the National Research Foundation (NRF) towards this research is hereby acknowledged. Opinions expressed, and conclusions arrived at, are those of the author and are not necessarily to be attributed to the NRF.

Compliance with Ethical Standards

Funding: This study was funded by the National Research Foundation (NRF) of South Africa (Grant no: 108533) and the Sugar Milling Research Institute.

Conflict of Interest: The authors declare that they have no conflicts of interest.

Ethical approval: This article does not contain any studies with human participants or animals performed by any of the authors.

References

Beauprez JJ, De Mey M and Soetaert WK (2010) Microbial succinic acid production: Natural versus metabolic engineered producers, Process Biochem. Elsevier Ltd, 45(7), pp. 1103–1114. doi: 10.1016/j.procbio.2010.03.035.

Bradfield MFA, Mohagheghi A, Salvachúa D, Smith H, Black BA, Dowe N, Beckham GT and Nicol W (2015) Continuous succinic acid production by *Actinobacillus succinogenes* on xylose - enriched hydrolysate, Biotechnol. Biofuels. BioMed Central, pp. 1–17. doi: 10.1186/s13068-015-0363-3.

Bradfield MFA and Nicol W (2014) Continuous succinic acid production by *Actinobacillus succinogenes* in a biofilm reactor: Steady-state metabolic flux variation, Biochem. Eng. J. Elsevier B.V., 85, pp. 1–7. doi: 10.1016/j.bej.2014.01.009.

Brink HG and Nicol W (2014) Succinic acid production with *Actinobacillus succinogenes* : rate and yield analysis of chemostat and biofilm cultures, pp. 1–12. doi: 10.1186/s12934-014-0111-6.

Costerton JW (1999) Introduction to biofilm, 11, pp. 217–221.

Ferone M, Raganati F, Olivieri G, Salatino P and Marzocchella A (2018) Continuous Succinic Acid Fermentation by *Actinobacillus succinogenes*: Assessment of Growth and Succinic Acid Production Kinetics, Appl. Biochem. Biotechnol. Applied Biochemistry and Biotechnology, (September). doi: 10.1007/s12010-018-2846-8.

Ferone M, Raganati F, Ercole A, Olivieri G, Salatino P and Marzocchella A (2018) Continuous succinic acid fermentation by *Actinobacillus succinogenes* in a packed-bed biofilm reactor,

Biotechnol. Biofuels. BioMed Central, 11:138 , pp. 1-11. https://doi.org/10.1186/s13068-018-1143-7.

González-García S, Argiz L, Míguez P and Gullón B (2018) Exploring the production of bio-succinic acid from apple pomace using an environmental approach, Chem. Eng. J. Elsevier, 350(May), pp. 982–991. doi: 10.1016/j.cej.2018.06.052.

van Heerden CD and Nicol W (2013) Continuous succinic acid fermentation by *Actinobacillus succinogenes*, Biochem. Eng. J. Elsevier B.V., 73, pp. 5–11. doi: 10.1016/j.bej.2013.01.015.

Heydorn A, Nielsen AT, Hentzer M, Givskov M, Ersbøll BK and Molin S (2000) Quantification of biofilm structures by the novel computer program COMSTAT, Microbiology, 146, pp. 2395–2407. doi: 10.1099/00221287-146-10-2395.

Hwang D and Lim YH (2015) Resveratrol antibacterial activity against *Escherichia coli* is mediated by Z-ring formation inhibition via suppression of FtsZ expression, Sci. Rep. Nature Publishing Group, 5(May), pp. 2–11. doi: 10.1038/srep10029.

Janissen R, Murillo DM, Niza B, Sahoo PK, Nobrega MM, Cesar CL, Temperini MLA, Carvalho HF, de Souza AA and Cotta MA (2015) Spatiotemporal distribution of different extracellular polymeric substances and filamentation mediate *Xylella fastidiosa* adhesion and biofilm formation., Sci. Rep., 5, p. 9856. doi: 10.1038/srep09856.

Jones TH, Vail KM and McMullen LM (2013) Filament formation by foodborne bacteria under sublethal stress, Int. J. Food Microbiol. Elsevier B.V., 165(2), pp. 97–110. doi: 10.1016/j.ijfoodmicro.2013.05.001.

Ki S, Lin C, Du C, Koutinas A, Wang R and Webb C (2008) Substrate and product inhibition kinetics in succinic acid production by *Actinobacillus succinogenes*, 41, pp. 128–135. doi: 10.1016/j.bej.2008.03.013.

Lee PC, Lee SY, Hong SH and Chang HN (2002) Isolation and characterization of a new succinic acid-producing bacterium, *Mannheimia succiniciproducens* MBEL55E, from bovine rumen., Appl. Microbiol. Biotechnol., 58(5), pp. 663–8. doi: 10.1007/s00253-002-0935-6.

Liu Y, Zheng P, Sun Z, Ni Y, Dong J and Wei P (2008) Strategies of pH control and glucose-fed batch fermentation for production of succinic acid by *Actinobacillus succinogenes* CGMCC1593, J. Chem. Technol. Biotechnol., 83(5), pp. 722–729. doi: 10.1002/jctb.1862.

Maharaj K, Bradfield MFA and Nicol W (2014) Succinic acid-producing biofilms of *Actinobacillus succinogenes*: Reproducibility, stability and productivity, Appl. Microbiol. Biotechnol., 98(17), pp. 7379–7386. doi: 10.1007/s00253-014-5779-3.

Marinho GS, Alvarado-Morales M and Angelidaki I (2016) Valorization of macroalga *Saccharina latissima* as novel feedstock for fermentation-based succinic acid production in a biorefinery approach and economic aspects, Algal Res. Elsevier B.V., 16, pp. 102–109. doi: 10.1016/j.algal.2016.02.023.

Mokwatlo SC and Nicol W (2017) Structure and cell viability analysis of *Actinobacillus succinogenes biofilms* as biocatalysts for succinic acid production, Biochem. Eng. J. Elsevier B.V., 128, pp. 134–140. doi: 10.1016/j.bej.2017.09.013.

Nghiem N, Kleff S and Schwegmann S (2017) Succinic Acid: Technology Development and Commercialization, Fermentation, 3(2), p. 26. doi: 10.3390/fermentation3020026.

Pateraki C, Patsalou M, Vlysidis A, Kopsahelis N, Webb C, Koutinas AA and Koutinas M (2016) *Actinobacillus succinogenes* : Advances on succinic acid production and prospects for development of integrated biorefineries, Biochem. Eng. J. Elsevier B.V., 112, pp. 285–303. doi: 10.1016/j.bej.2016.04.005.

Pelayo-ortiz C and Corona-gonza RI (2008) Kinetic study of succinic acid production by *Actinobacillus succinogenes* ZT-130, 43, pp. 1047–1053. doi: 10.1016/j.procbio.2008.05.011.

Riverdia (2018) *No Title*. Available at: https://reverdia.com/ (Accessed: 7 December 2018).

Salvachúa D, Mohagheghi A, Smith H, Bradfield MFA, Nicol W, Black BA, Biddy MJ, Dowe N and Beckham GT (2016) Succinic acid production on xylose-enriched biorefinery streams by *Actinobacillus succinogenes* in batch fermentation., Biotechnol. Biofuels. BioMed Central, 9(1), p. 28. doi: 10.1186/s13068-016-0425-1.

Samuelov N, Datta R, Jain M and Zeikus J (1999) Whey fermentation by *Anaerobiospirillum succiniciproducens* for production of a succinate-based animal feed additive, Appl. Environ. Microbiol., 65(5), pp. 2260–3.

Schneider CA, Rasband WS and Eliceiri KW (2012) NIH Image to ImageJ: 25 years of Image Analysis HHS Public Access, Nat. Methods, 9(7), pp. 671–675. doi: 10.1038/nmeth.2089.

Scholten E, Renz T and Thomas J (2009) Continuous cultivation approach for fermentative succinic acid production from crude glycerol by *Basfia succiniciproducens* DD1., Biotechnol. Lett., 31(12), pp. 1947–51. doi: 10.1007/s10529-009-0104-4.

Shen N, Zhang H, Qin Y, Wang Q, Zhu J, Li Y, Jiang MG and Huang R (2018) Efficient production of succinic acid from duckweed (Landoltia punctata) hydrolysate by *Actinobacillus succinogenes* GXAS137, Bioresour. Technol., 250(August 2017), pp. 35–42. doi: 10.1016/j.biortech.2017.09.208.

Song H and Lee SY (2006) Production of succinic acid by bacterial fermentation, Enzyme Microb. Technol., 39(3), pp. 352–361. doi: 10.1016/j.enzmictec.2005.11.043.

Urbance SE, Pometto AL, Dispirito A a and Denli Y (2004) Evaluation of succinic acid continuous and repeat-batch biofilm fermentation by *Actinobacillus succinogenes* using plastic composite support bioreactors., Appl. Microbiol. Biotechnol., 65(6), pp. 664–70. doi: 10.1007/s00253-004-1634-2.

Yan Q, Zheng P, Tao ST and Dong JJ (2014) Fermentation process for continuous production of succinic acid in a fibrous bed bioreactor, Biochem. Eng. J. Elsevier B.V., 91, pp. 92–98. doi: 10.1016/j.bej.2014.08.002.

Zheng P, Dong J-J, Sun Z-H, Ni Y and Fang L (2009) Fermentative production of succinic acid from straw hydrolysate by *Actinobacillus succinogenes*., Bioresour. Technol. Elsevier Ltd, 100(8), pp. 2425–9. doi: 10.1016/j.biortech.2008.11.043.

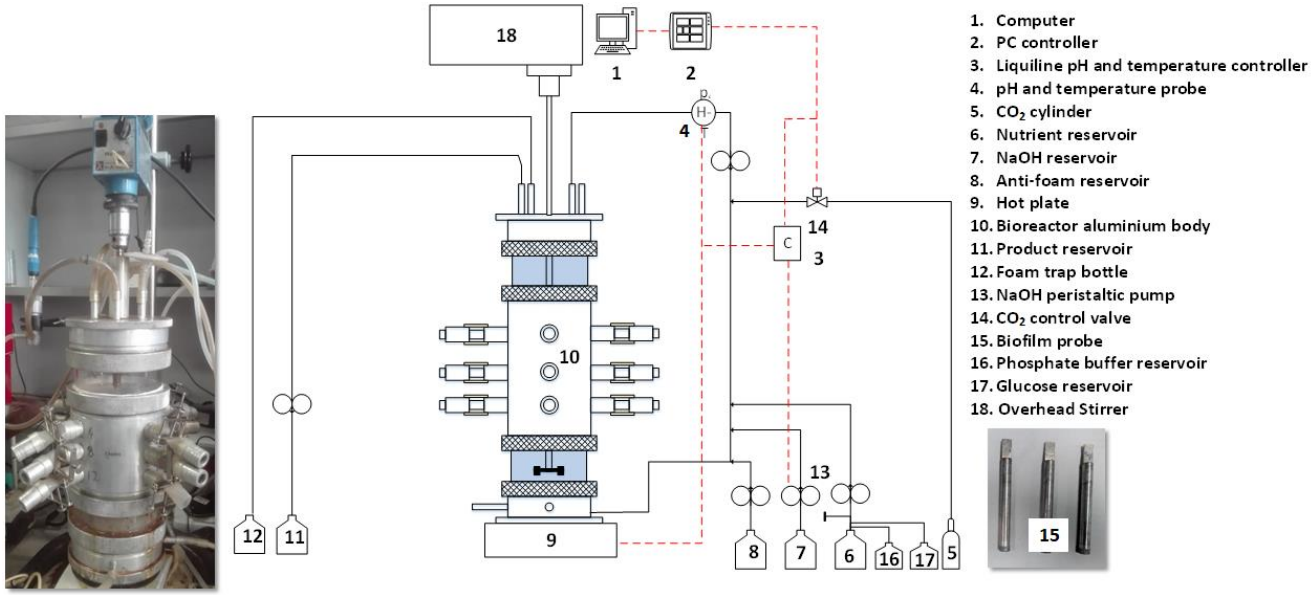
18
1
2
4
14
3
10
13
12
11
9
8
7
6
16
17
5
15
1. Computer
2. PC controller
3. Liquiline pH and temperature controller
4. pH and temperature probe
5. CO_2 cylinder
6. Nutrient reservoir
7. NaOH reservoir
8. Anti-foam reservoir
9. Hot plate
10. Bioreactor aluminium body
11. Product reservoir
12. Foam trap bottle
13. NaOH peristaltic pump
14. CO_2 control valve
15. Biofilm probe
16. Phosphate buffer reservoir
17. Glucose reservoir
18. Overhead Stirrer

Figure 1

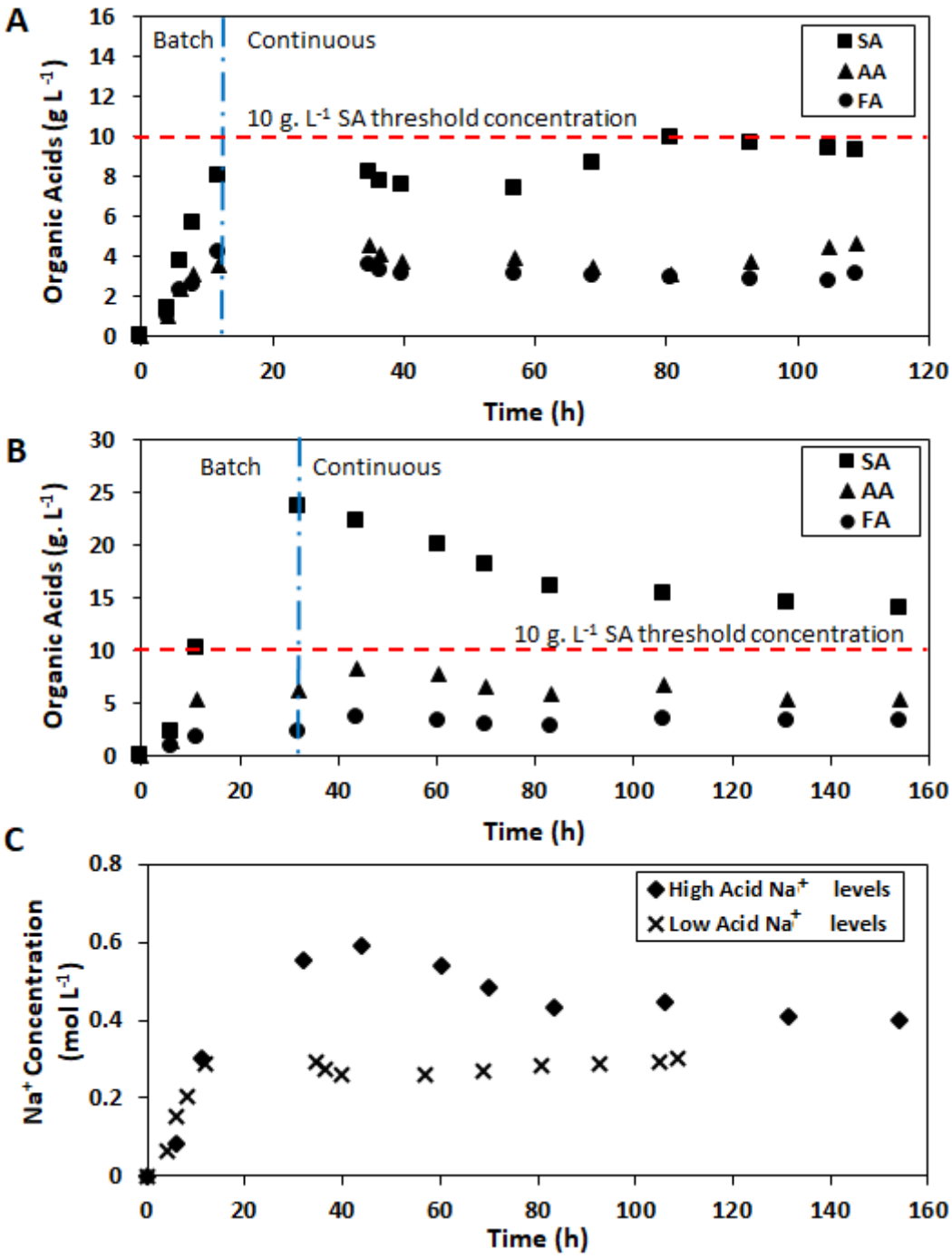
A
Batch
Continuous
SA
AA
FA
10 g. L-1 SA threshold concentration
Organic Acids (g L-1)
Time (h)
B
Batch
Continuous
SA
AA
FA
10 g. L-1 SA threshold concentration
Organic Acids (g. L-1)
Time (h)
C
High Acid Na+ levels
Low Acid Na+ levels
Na+ Concentration (mol L-1)
Time (h)

Figure 2

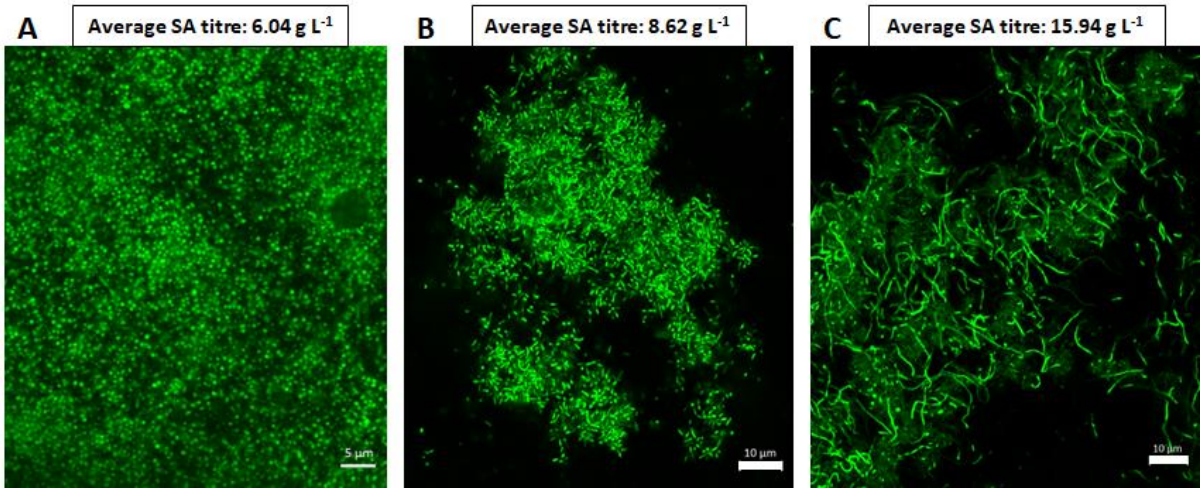

Figure 3

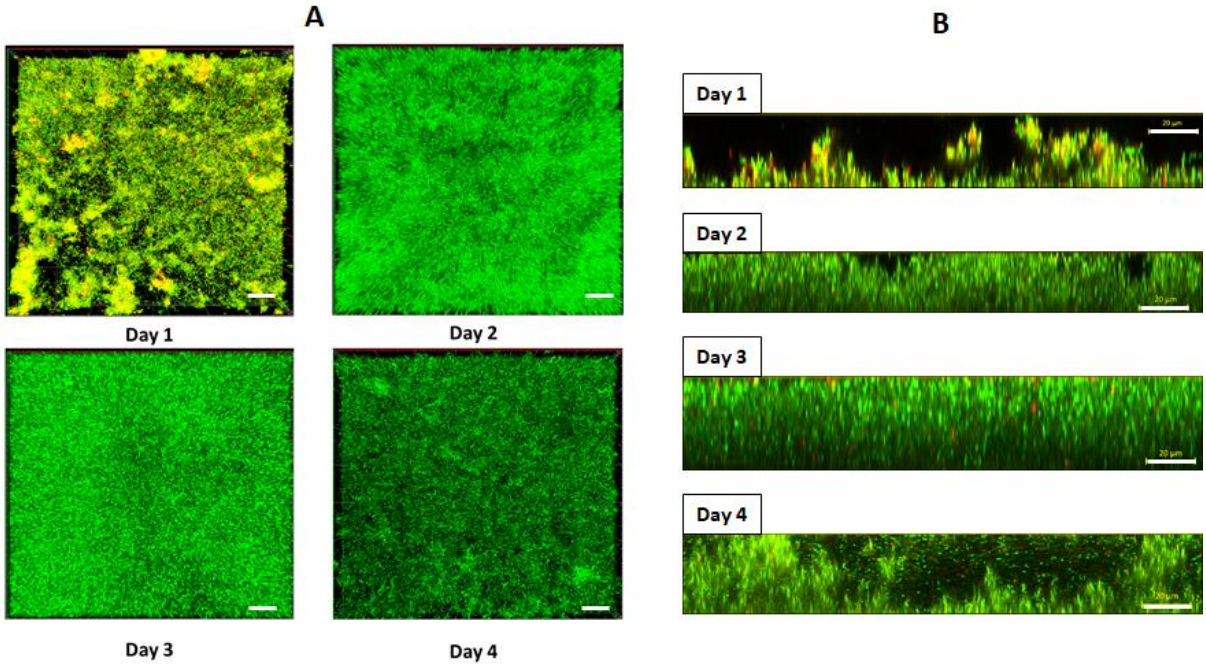

Figure 4

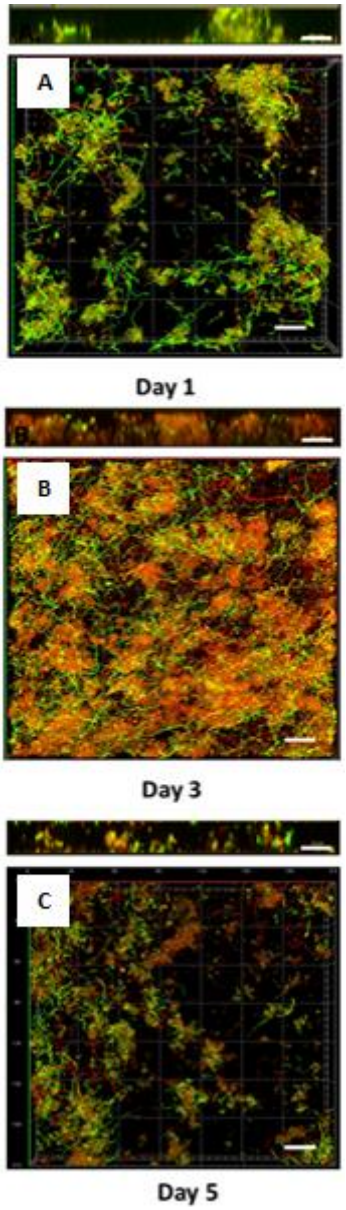

Figure 5

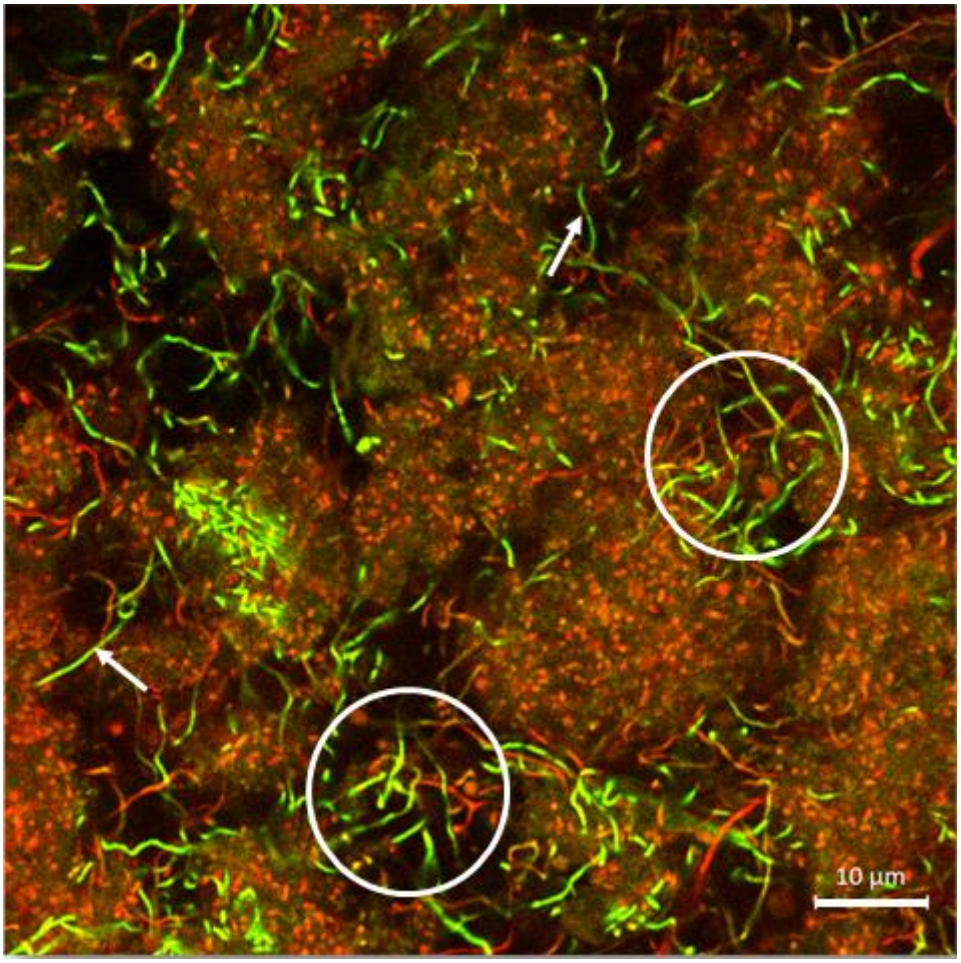

Figure 6

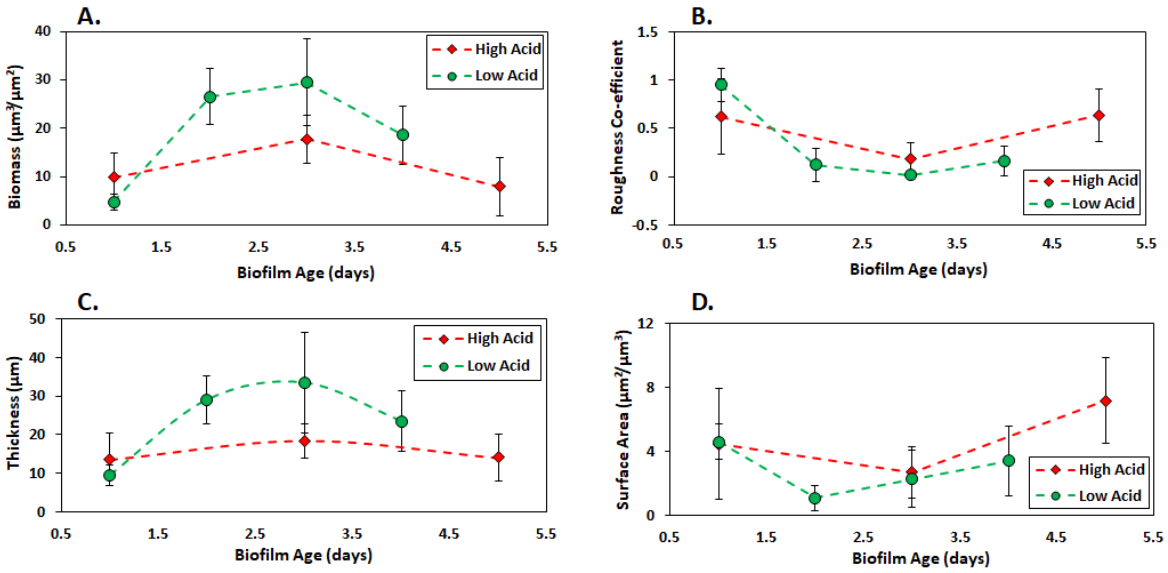

Figure 7

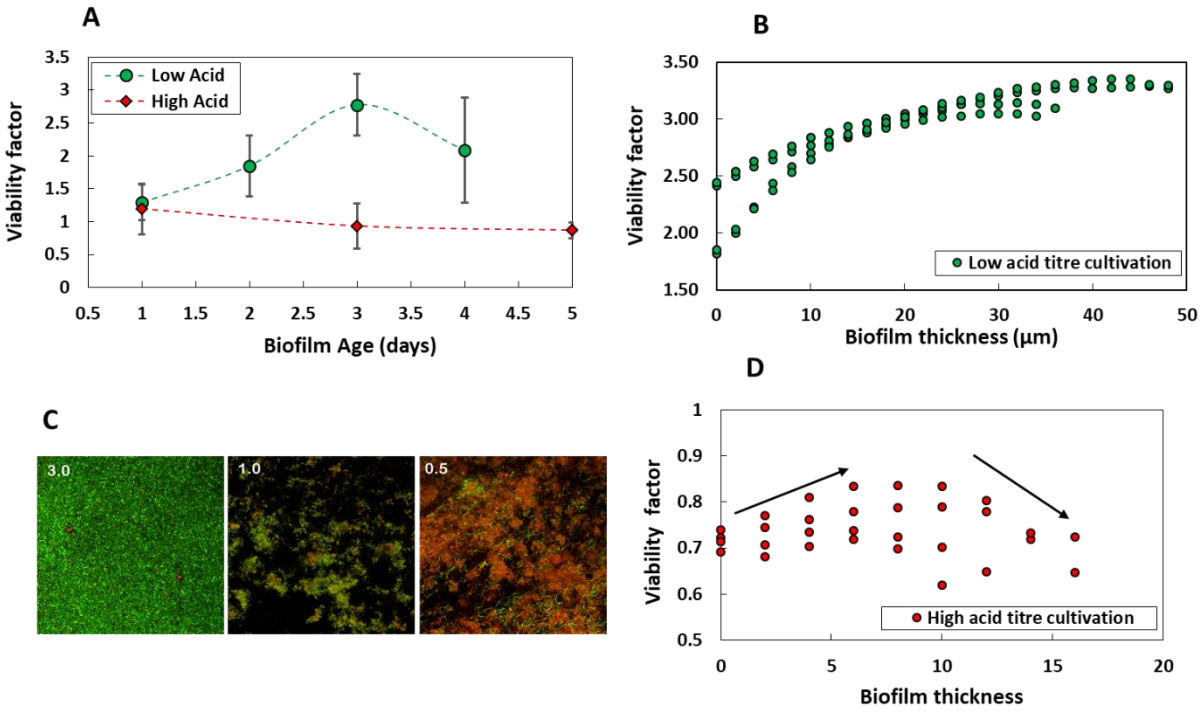
A
Low Acid
High Acid
Viability factor
Biofilm Age (days)
B
Viability factor
Low acid titre cultivation
Biofilm thickness (µm)
C
3.0
1.0
0.5
D
Viability factor
High acid titre cultivation
Biofilm thickness

Figure 8

Table 1: A statistical comparison of biofilm viability for growth at low and high accumulation conditions.

Biofilm Age	Biofilm Cultivation Conditions				Statistical Comparison		
	HA		LA				
	Mean Viability Factor	Samples	Mean Viability Factor	Samples[1]	P value	Difference between means	Comment
Day 1	1.193 ± 0.027	203	1.292 ± 0.014	347	0.0004	0.099 ± 0.028	Means are significantly different (P< 0.05)
Day 3	0.933 ± 0.018	344	2.771 ± 0.025	358	0.0001	1.838 ± 0.031	Means are significantly different (P< 0.05)

[1] Refers to the number of *xy* plane optical scan images of the biofilm processed for a particular day of biofilm sampling.

Figure Captions

Figure 1: The continuous fermentation setup used for biofilm cultivation, the setup allowed for multiple sterile sampling of biofilm coupons.

Figure 2: Metabolite concentration profiles for biofilm cultivation at low accumulation conditions (**A**) and at high accumulation conditions (**B**). The build-up of sodium levels in the bioreactor at both low and high accumulation condition is shown in (**C**). The sodium concentrations were calculated from the acid concentrations assuming neutralisation as pH was controlled at 6.8.

Figure 3: The different cell morphologies expressed by *Actinobacillus succinogenes* in biofilms grown under varying succinic acid titre conditions. In (**A**), under lower SA titre conditions, biofilm cells where mostly cocci shaped, whereas in (**B**) cells started to exhibit a classic bacillus rod-like shape as the SA growth concentration increased slightly. Growing at high SA concentrations (**C**) biofilm cells were drastically elongated although clumps of cocci cells were observed. The scale bar indicates 5 μm in (**A**) and 10 μm in (**B**) and (**C**)

Figure 4: Representative *xy-plane* (**A**) and *xz-plane* (**B**) views of the biofilm development at low SA titre conditions over a period of four days. The biofilm rapidly achieved a complete basal coverage on the first day though microcolonies were irregular in height and size. Over the course of the next two days, the biofilm uniformly increased in thickness with minimal voids noticeable between microcolonies throughout the biofilm thickness. The scale bars indicate 20 μm.

Figure 5: Biofilm development at high SA acid titres as represented by *xy-plane* and *xz-plane* images. A patchy biofilm with low surface coverage was observed on the first day with a cluster of cell microcolonies interconnected by a network of elongated cells. On the third day the biofilm was less patchy as microcolony structures were closely spaced whilst the network of elongated cells was much denser. Shedding of biofilm resulted in a patchy structure on the fifth day. The scale bars indicate 20 μm.

Figure 6: Cell clusters surrounded by filamentous cells. Filamentous cells were were mostly located in-between the borders of neighbouring cell clusters (indicated by white circles) and were protruding out of cell clusters and entering other neighbouring cell clusters (indicated by white arrows) as if interconnecting cell clusters. The scale bars indicate A0 μm.

Figure 7: A quantitative comparison of biofilm parameters for biofilm grown in low and high SA environments. It is apparent that biofilm experiences high growth rates at low SA titres as shown by rapid increases in biomass volume per area (**A**) and thickness (± 10 μm per day) (**C**) when compared to growth at high acid conditions wherein the biofilm struggles to grow. The patchy structure of the biofilm grown at high acids environments results in high exposed biofilm surface area per volume needed at these harsh conditions. The quantitative data is consistent with observations from the qualitative image analysis.

Figure 8: The activity of the biofilm during low acid titre and high acid titre (**A**) biofilm development. A higher green to red colour intensity correlates to images were cells were mostly active (green). Biofilm grown at low acid titres was mostly active throughout its development, whereas that grown in high acids environment become increasingly inactive even resulting in excessive shedding. This is supported by steady state biofilm activity fractions investigated at varying acid concentrations (**B**).